IJBPAS, January, Special Issue, 2022, 11(1): 697-710

ISSN: 2277–4998

International Journal of Biology, Pharmacy and Allied Sciences (IJBPAS)

'A Bridge Between Laboratory and Reader'

www.ijbpas.com

CLIMATE RISK DETECTION AND PRIORITIZATION OF SUB-WATERSHEDS OF THE AGRANI RIVER BASIN USING FUZZY-ANALYTICAL HIERARCHY PROCESSES

ANIL SS[*1] & DAS SA[2]

1: Division of Geoinformatics, Dept. of Water & Health, JSS Academy of Higher Education & Research, Mysore, 570 015, India

2: Department of Studies in Geography, University of Mysore, Mysuru-06

[*]**Corresponding Author: Dr. Sawant Sushant Anil; E Mail: geo_sushant@jssuni.edu.in**

Received 10th June 2021; Revised 11th July 2021; Accepted 20th Aug. 2021; Available online 15th Jan. 2022

https://doi.org/10.31032/IJBPAS/2022/11.1.1084

ABSTRACT

Drylands are significantly affected by climate change through changing spatial- temporal distribution of the climatic variables thus making these areas prone to the climate risk. Climatic risk adaptation is essential through various resource management activities, appropriate policymaking, capacity-building institutions, and individuals. This can be achieved by prioritizing areas for climatic risk adaptation and mitigation. The comprehensive study and inclusion of various climatic variables in watershed management increase the success of conservation practices and management. Therefore, with climate risk, there are new challenges to ensure that watershed management also leads to climate risk adaptation and mitigation.

The current study offers the Fuzzy Analytical Hierarchical Process as an effective multicriteria decision support model (MCDSM) for identifying and prioritizing the Agrani River's Climate-Risk sub-watersheds. The methodology was created by combining the Fuzzy-AHP method, basin climate risk analysis, and a Geographic Information System (GIS). The final score produced from the Fuzzy-AHP procedure was used to assign ranks to all sub-watersheds. For the Climate Change Mitigation & Management, these sub-watersheds were prioritized into five categories based on Fuzzy-AHP scores:

very low, low, medium, high, and very high.

The result illustrates the nine sub-watersheds covering approximately 35% of the watershed area prone to climate risk thus given high to very high priority and 15.47 % area has shown moderate climate risk.

This study suggests that the fuzzy-AHP model, Climate-Risk Analysis, and GIS technique may be utilized effectively to identify and prioritize critical sub-watersheds for climate change mitigation and management.

Keywords: Climate Risk, Fuzzy-Analytical Hierarchy Processes, Mann Kendall Trend Test, Prioritization

INTRODUCTION

Drylands are significantly affected by climate change through changing spatial-temporal distribution of the climatic variables such as rainfall, temperature, evapotranspiration, and wind speed. The changes in the pattern of such climatic variables affect the degree of dryness in the dryland region and accelerate land degradation that is referred to in drylands as desertification. This climate change would also change soil water availability, significantly influencing ecosystems' functioning in water-stressed dryland ecosystems and thus dryland become prone to climatic risk.

It is predicted that climate risk will significantly affect the agricultural sector in the dryland region, reducing agricultural yields. A study led by Washington State University has reported that the drylands worldwide will grow at an accelerating rate due to potential climate change and will likely reduce average productivity (Yao *et al*. 2020).

Climatic risk adaptation is essential through various resource management activities, appropriate policymaking, capacity-building institutions, and individuals. This can be achieved by prioritizing areas for climatic risk adaptation and mitigation.

One of the basic components to meticulously address the water stress is through watershed management and it is also one of the universally accepted approaches for natural resource management and conservation. While carrying out integrated watershed management, comprehensive inclusion is essential. Most integrated watershed management studies are based on land and water resources while neglecting the climatic variables. The comprehensive study and inclusion of various climatic variables in watershed management increase the success of conservation practices and management. Therefore, with climate risk, there are new challenges to ensure that watershed management also leads to climate risk adaptation and mitigation.

Therefore, the aim of this research objective is to investigate the spatial-temporal variation in patterns of climatic variables, evaluate their effects on drylands, and prioritize the SWs for climate risk adaptation and mitigation.

METHODOLOGY

According to the review of literature pertaining to the watershed management most of the studies have been confined to land and water resources neglecting climatic variables. From this point of view the present study has been examined adding climatic variables and to prioritise the SWs, Fuzzy logic has been applied to obtain greater clarity in understanding the exact land under climate risk.

The climatic analysis and the prioritization of the sub-watersheds for climate risk adaptation and mitigation have been carried out through an integrated approach of statistical analysis, Geospatial technology, and Fuzzy Analytical Hierarchical Process (Fuzzy-AHP). To fulfil the study's goals and objectives, a multi-tiered technique consisting following steps was used:

i. Climatic data collection and preparation of the geodatabase

ii. Spatial-temporal analysis of climatic variables at the watershed and SW level, Application of the fuzzy-AHP for deriving weights and ranks of the climatic parameters and its classes,

iii. Prioritization of the SWs to mitigate climate risk using fuzzy- AHP.

The materials and procedures utilized in this study are described in detail below and represented in Figure 1.

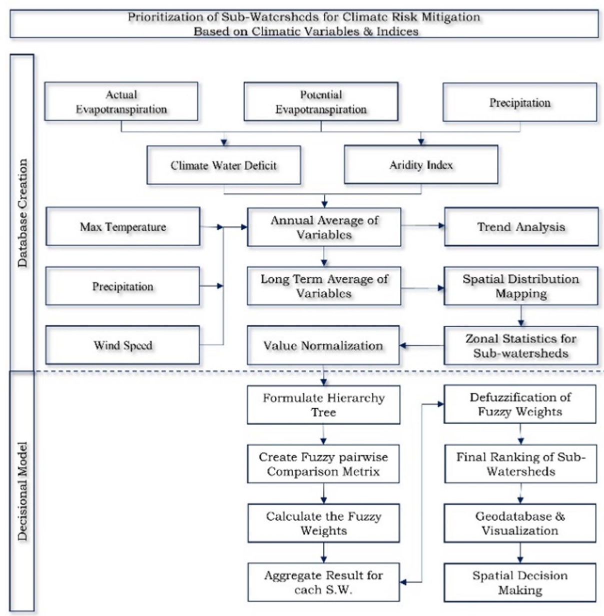

Figure 1: Methodology Flowchart

Climate Database Preparation

The monthly rainfall, maximum temperature, potential evapotranspiration, wind speed, and Climate Water Deficit (CWD) dataset of 58 years (1961–2018) was used in the analysis which were obtained from the Terraclimate dataset (http://www.climatologylab.org). The average annual and long-term average dataset for the study area was computed from the monthly dataset. The selected climatic variables can effectively be used to study the degree of dryness and the intensity of climate risk. The spatial distribution and linear trend analysis of the variables over the last 58 years (1961-2018) were studied using statistical methods and geospatial technology.

Computation of the Climatic Variables and Indices.

The following five climatic variables are identified as climate risk parameters such as

i) Aridity Index (AI),
ii) Maximum Temperature,
iii) Wind Speed,
iv) Climatic Water Deficit (CWD),
v) Rainfall.

The Fuzzy-AHP method has been used to prioritize sub-watersheds to effectively mitigate climate risk and study the level of dryness at the sub-watershed level. The fuzzy matrix weights were computed using Buckley's (1985) Geometric Mean Method. Following that, the final fuzzy weights for SWs were calculated by combining all fuzzy matrix fuzzy weights. Using the final fuzzy ratings, the SWs were ranked from highest to lowest.

The pairwise comparison matrices were constructed using all five climatic parameters and sub-classes of each parameter. After that, composite weights were computed for each climatic parameter in use. The resulted Fuzzy-AHP score has been utilized to rank the sub-watersheds based on their degree of dryness. The Fuzzy-AHP score integrated with the spatial data in ArcGIS Pro software for mapping sub-watershed prioritization. All the SWs were classified into five priority categories, which can be used while planning climate risk mitigation at the sub-watershed level.

Result and Discussion

Spatial-Temporal Analysis of The Climatic Variables

Maximum Temperature

The pattern of temperature is extremely variable in the dryland region. All the seasons have significant diurnal temperature fluctuations that restrict the growth of vegetation and increases evapotranspiration. In the current analysis, the maximum temperature was considered by retaining a climate risk perspective. The maximum temperature data is useful while studying the degree of dryness, health and tolerance level of the plants, length of growing season, & evapotranspiration rate.

The long-term change in maximum temperature is depicted in the graph (Figure 2) with a trendline equation y = mx + b where the slope is m, and the y-intercept is b. In this graph, a slope depicts an average annual increase in temperature over the 58 years (1961 to 2018), which is 0.232°C per year. Though the maximum temperature increase is gradual over time, it is likely to be decisive for the dryland region's future environmental condition. The spatial distribution of the long-term (1961-2018) average annual maximum temperature is mapped in the figure 5. The average, lowest and highest maximum average annual temperature is 31.68°C, 30.72°C, and 32.58°C, respectively. The highest (32.19°C) and lowest maximum (31.06°C) temperature is recorded in the SW18 and SW3.

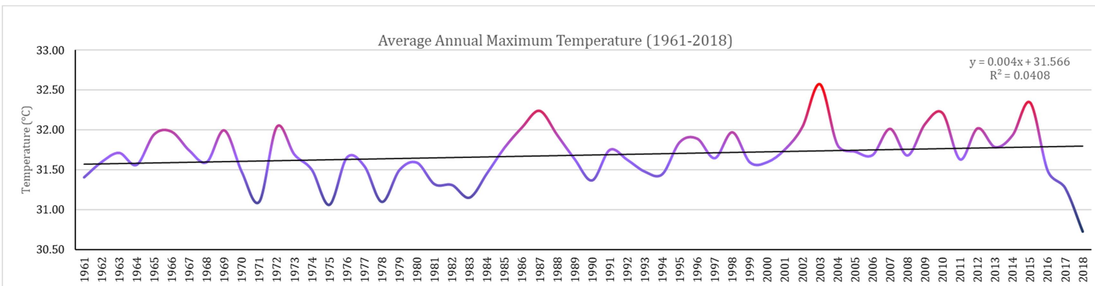

Figure 2: Average Annual Maximum Temperature (1961-2018)

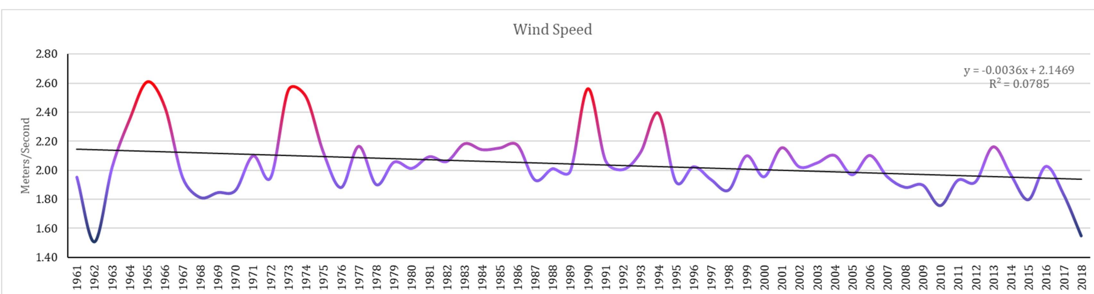

Figure 3: Average Annual Wind Speed (1961-2018)

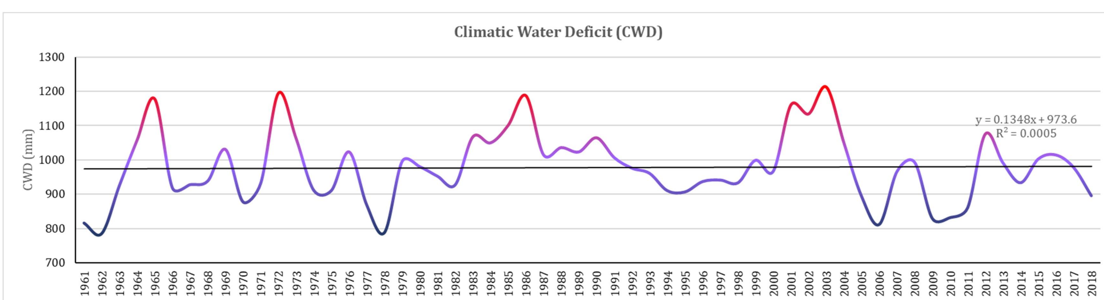

Figure 4: Average Annual Climatic Water Deficit(1961-2018

Wind Speed

The wind is a significant climatic factor that intensifies soil erosion, causes extreme atmospheric drought and damage growing plants. The primary reason for the widespread severe wind erosion in the dryland was the temporal mismatch between wind speed and vegetation coverage. The monthly wind speed (m/s) data is procured and used to derive the long-term average annual wind speed and yearly time series dataset. The mean annual wind speed was computed for the entire Agrani watershed and the sub-watersheds for the 58 years (1961-2018).

An average wind speed over the Agrani river watershed is 2.04 m/s. The lowest (1.99 m/s) and highest (2.12 m/s) annual mean wind speed were recorded over SW10 and SW18. The mean wind speed representing the long-term climate have computed using yearly mean wind speed data (1961-2018).

A trendline of the surface wind speed is illustrated in graph (Figure 3) that shows declining trend (0.2088 m/s) from 1961 to 2018. This may be due to the increased surface roughness by the change in the land use land cover (LULC) and the change in the thermal gradient. Differences in temperature variations drive air movements at various locations. The more significant the difference between cold and warm air, the stronger the wind will be. The weakening of this gap is one consequence of global warming (McVicar *et al*. 2012). Some studies have concluded that the Indian subcontinent is also expected to have decrease wind speed (Eichelberger *et al*.).

Climatic Water Deficit (CWD)

Climatic Water Deficit (CWD) quantifies annual evaporative demand that exceeds available water (Flint and Flint 2012). It is calculated as the difference between actual evapotranspiration (*AET*) and potential evapotranspiration (PET) (Abatzoglou *et al*., 2018).

$$D = PET - AET \qquad 1.1$$

Where D = Climatic Water Deficit.

PET = Potential Evapotranspiration,

AET = Actual Evapotranspiration,

It is strongly correlated with the distribution of vegetation in a landscape and is thus an index of potential effects of drought stress on plants. It is also considered a significant parameter for quantifying the relationship between climate and crop yield (Prăvălie *et al*. 2014). The CWD is higher in the dryland areas than anywhere else, so it is a reliable indicator for examining climate risk.

The spatial distribution of long-term (1961-2018) average annual CWD is mapped in the Figure 5). The average, lowest and highest average yearly CWD is 977.58 mm, 944.80 mm, and 1028.29 mm. The highest (1028.29mm) and lowest (944.80mm) CWD is recorded in the SW18 and SW10.

The average annual CWD trend is illustrated in the graph (Figure 4) that shows the gradual increase (7.82 mm) in the CWD from 1961 to 2018. The rise in CWD values over 58 years reveals the increased dryness in the environment. This trend of CWD will continue since the temperature is rising which will lead to have change in vegetation stress level, soil moisture, groundwater availability, and cropping pattern. Thus, CWD is an essential indicator of desertification, and its understanding can effectively be used to tackle climate risk mitigation at the sub-watershed level.

Aridity Index (AI)

According to United Nations Environmental Programme (UNEP), the aridity index is defined as the degree of climatic dryness in correspondence to the ratio of annual mean precipitation (P) to the yearly mean potential evapotranspiration (PET).

The AI is useful for identifying the exact location in a region and is useful for delimiting the areas suffering from a lack of water.

The AI value provides to understand the degree of dryness and vice versa. It means lower the AI higher the degree of dryness, and the higher the AI lower the degree of dryness. The formula (Eq.1.2) for the computation of the AI is given below.

$$AI = \frac{P}{PET} \tag{1.2}$$

The degree of aridity values has been classified into five levels as follows (Table 1).

Table 1 UNEP aridity index classification

Climate Type	Aridity Index
Dryland Subtypes	
Hyper-arid	AI < 0.05
Arid	0.05 ≤ AI < 0.20
Semi-Arid	0.20 ≤ AI <0.50
Dry Subhumid	0.50 ≤ AI < 0.65
Non-Dryland	
Humid	AI ≥ 0.65

The climate's dryness can adversely affect water availability, the ecosystem's health, agricultural production, and livestock health. Thus, when managing watershed resources, it is essential to consider AI. In this study, a quantitative assessment of terrestrial aridity distribution over 1961–2018 has carried out for the study area.

The spatial distribution of average AI is mapped for 1961-2018 (Figure 5). According to the UNDP classification of AI, the Agrani river watershed falls under the semi-arid region. The average, lowest and highest AI is 0.266, 0.229, and 0.310, respectively. The lowest (0.229) and highest (0.310) AI is recorded over the SW22 and SW8, respectively. The increased temperature and decreased trend of rainfall indicate that if proper management practices are not implemented, the degree of dryness would increase.

Rainfall Analysis

In dryland regions, where rainfed agriculture is practiced, the spatial-temporal study of rainfall is essential to understand its effect on the economy and the dryland ecosystem. In this research study, more emphasis was given on rainfall analysis due to its intense effect on the dryland region: the rainfall distribution and trend manifest change and variation in other climatic parameters. Therefore, annual rainfall distribution has studied using long-term average rainfall.

Annual Rainfall Distribution

The spatial distribution of the long-term (1961-2018) average annual rainfall is mapped in the Figure 6. The long-term (1961-2018) average annual rainfall within the study area is 862.27 mm with a standard deviation of 87.76 mm. However, an average yearly rainfall's spatial distribution varies from 700 mm over the Southern part to slightly more than 1182 mm over the eastern region during observation period. The lowest and highest average annual rainfall within sub-watersheds is recorded within SW22 (727.63 mm) and SW8 (1003.94 mm), respectively. Due to semi-arid climate and its location on the eastern side of the western ghat, this area comes under the rain shadow region. Since almost 72% of the annual rainfall occurs during the south-west monsoon season, rainfed agriculture is prevalent and therefore seasonal distribution of the rainfall is essential to study.

3.2 Prioritization of Sub-watersheds for Climate change Mitigation & Management

The Fuzzy-AHP approach was used with five climate parameters to prioritize sub-watersheds of the Agrani River for climate risk reduction. The climatic parameters such as aridity Index, Climatic Water Deficit (CWD), Rainfall, Maximum Temperature, and wind speed can effectively be used to study the climate risk and degree of dryness over the semi-arid region. The average annual values of the climatic variables for SWs are shown below (Table 2).

By assigning Triangular Fuzzy Numbers, uncertainty in prioritizing climatic indicators based on their influence on climate risk and aridity has been eliminated (TFN). To assign scores to the climatic parameters, the TFN conversion scale was used. The relationship between climatic parameters and the risk of aridity can assist us in identifying climate risk-prone SWs. The degree of dryness is positively associated to climatic parameters such as Climatic Water Deficit (CWD), Maximum Temperature, and wind speed. As a result, the higher the value of such climatic parameters, the higher the rank in the priority process.

On the contrary, the climatic parameters such as Rainfall & Aridity Index are inversely related to the degree of dryness. Hence, rainfall and Aridity Index values were inversed in the matrix of climatic parameters. Thus, each of the twenty-two SW parameters was assigned a rank based on its influence on the risk of aridity and thus climate risk. Before creating a pairwise comparison matrix, the climatic values were normalised. This matrix (Table 4) was constructed while considering each climatic parameter's relative significance with other parameters.

The SWs were prioritized using the final Fuzzy-AHP score, which ranged from 0.0125 to 0.0819 (Table 5). The SW8 was received the first rank with the highest Fuzzy-AHP score (0.0819) in terms of the degree of dryness.

Table 2: Actual Values of Climatic Variables

SWs	CWD	Max Temp (̊C)	Wind Speed (m/s)	Rainfall (mm)	Aridity Index
SW1	971.96	31.87	2.03	934.44	0.29
SW2	957.99	32.05	2.01	990.41	0.31
SW3	944.80	31.06	2.03	846.91	0.27
SW4	976.35	31.52	2.05	815.80	0.26
SW5	958.00	31.33	2.04	887.74	0.28
SW6	983.39	31.72	2.05	814.30	0.26
SW7	993.19	32.05	2.07	897.08	0.28
SW8	950.59	31.91	2.01	1003.9	0.31
SW9	991.65	31.73	2.04	839.44	0.26
SW10	990.15	31.76	1.99	826.85	0.26
SW11	1001.37	32.03	2.04	857.64	0.27
SW12	987.57	32.01	2.03	918.44	0.28
SW13	1021.56	32.15	2.04	811.81	0.25
SW14	1000.01	32.17	2.05	866.71	0.27
SW15	957.49	31.79	2.10	977.07	0.30
SW16	1014.56	32.10	2.04	798.20	0.25
SW17	1014.18	31.92	2.01	783.56	0.24
SW18	1013.78	32.19	2.12	826.77	0.25
SW19	1028.29	32.00	2.07	748.80	0.23
SW20	999.70	31.79	2.10	793.38	0.25
SW21	987.44	31.56	1.99	774.72	0.24
SW22	1012.70	31.56	2.06	727.63	0.23

Table 3: Normalized Values of Climatic Variables

SWs	CWD	Max Temp (̊C)	Wind Speed (m/s)	Rainfall (mm)	Aridity Index
SW1	0.945	0.990	0.960	0.069	0.063
SW2	0.932	0.996	0.947	0.013	0.008
SW3	0.919	0.965	0.956	0.156	0.122
SW4	0.949	0.979	0.966	0.187	0.169
SW5	0.932	0.973	0.963	0.116	0.095
SW6	0.956	0.985	0.967	0.189	0.169
SW7	0.966	0.996	0.979	0.106	0.096
SW8	0.924	0.991	0.946	0.000	0.000
SW9	0.964	0.986	0.961	0.164	0.151
SW10	0.963	0.987	0.939	0.176	0.161
SW11	0.974	0.995	0.962	0.146	0.142
SW12	0.960	0.995	0.956	0.085	0.088
SW13	0.993	0.999	0.964	0.191	0.194
SW14	0.972	1.000	0.968	0.137	0.138
SW15	0.931	0.988	0.990	0.027	0.025

SW16	0.987	0.997	0.961	0.205	0.204
SW17	0.986	0.992	0.950	0.220	0.215
SW18	0.986	1.000	0.999	0.176	0.187
SW19	1.000	0.994	0.975	0.254	0.251
SW20	0.972	0.988	0.989	0.210	0.206
SW21	0.960	0.981	0.940	0.228	0.216
SW22	0.985	0.980	0.970	0.275	0.264

Table 4: Pairwise Comparison Matrix

	Aridity Index			CWD			Rainfall			Max Temperature			Wind Speed			Fuzzy Weights
AI	1	1	1	1	2	3	3	4	5	4	5	6	5	6	7	0.4303
CWD	0.33	0.50	1	1	1	1	2	2	4	3	4	5	4	5	6	0.2899
Rainfall	0.20	0.25	0.33	0.25	0.50	0.50	1	1	1	2	3	4	3	4	5	0.1521
Max Temp	0.17	0.20	0.25	0.20	0.25	0.33	0.25	0.33	0.50	1	1	1	2	3	4	0.0818
Wind Speed	0.14	0.17	0.20	0.17	0.20	0.25	0.20	0.25	0.33	0.25	0.33	0.50	1	1	1	0.0459

Likewise, The Fuzzy-AHP score was used to rank all SWs. As a result, the SWs with the highest rank were given the highest priority in mitigating the climatic risk.

Further, all SWs were categorized to determine SWs, which were similar in the climatic risk. The equal interval classification method was used to determine Fuzzy-AHP score arrangement into five classes. Based on the Fuzzy-AHP scores, the Agrani river's twenty-two sub-watersheds were classified into five climatic risk classes. (Table 6) such as: very high (0.0681-0.0819), high (0.0543-0.680), moderate (0.0404-0.0542), low (0.0265-0.0403), and very low (≤ 0.0264).

SW8, SW2, and SW15 have a very high climatic risk, according to the final priority ratings of all SWs, with a Fuzzy-AHP score of 0.0681.and requires intensive preparedness to mitigate the climatic risk. Because of the high potential-evaporation, CWD, wind speed, and less rainfall and aridity index in these SWs, it is particularly vulnerable to climate risk and hence falls under a very high priority zone. The next highly risk sub-watersheds with the Fuzzy-AHP score range of 0.0543-0.680 are SW1, SW7, SW12, SW13, SW19, and SW14 and need the attention and preparedness to lower the climatic risk. Moderate priority was given to the SW11, SW18, SW16, and SW5, with the Fuzzy-AHP score, ranged from 0.0404-0.0542. SWs with high rainfall and low evapotranspiration due to extensive plant cover had a lower Fuzzy-AHP score, putting them in the low to very low priority zone. Approximately 34.94 percent of the watershed area (674.05 km2) is covered by high to very high prioritized SWs, while nearly 15.47 percent of the watershed area (298.42 km2) is covered by moderately prioritized SWs. A total of nine SWs covers 49.60 percent of the Agrani watershed, with 956.90 km2 categorized as low to extremely low priority zones. In addition, the spatial data and Fuzzy-AHP scores of all SWs were imported into the ArcGIS Pro software for mapping and prioritizing the climatic risk prone SWs for spatial planning to minimize and reduce climatic risk in the area. (Figure 7).

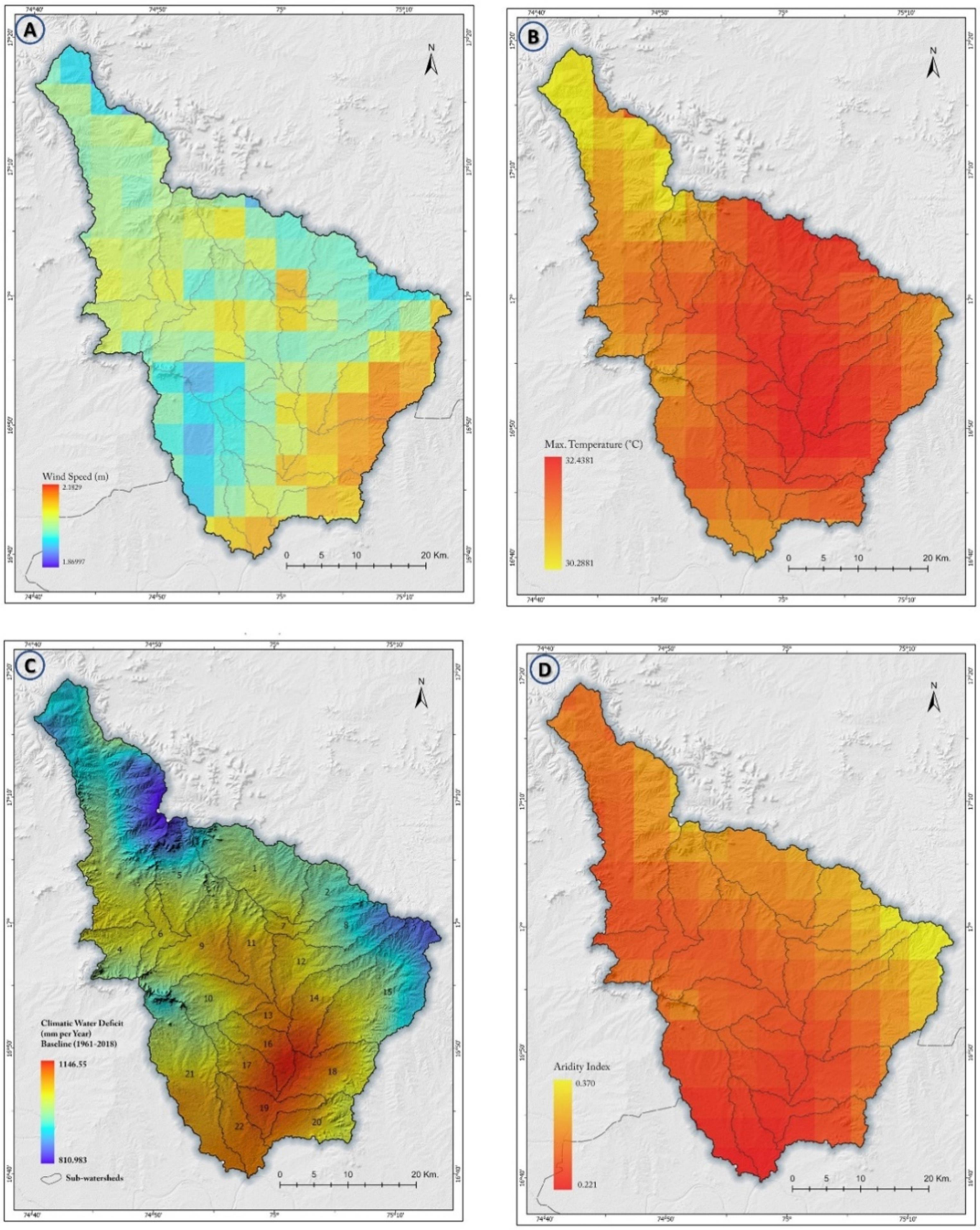

Figure 5a) Average Annual Wind Speed (mm), b) Average Annual Maximum Temperature, c) Average Annual Climatic Water Deficit, d) Aridity Index (1961-2018)

Table 5: Fuzzy-AHP ranks of the sub-watersheds

SW Name	SW 8	SW 2	SW 15	SW 1	SW 7	SW 12	SW 13	SW 19	SW 14	SW 18	SW 11
FAHP Score	0.0819	0.0769	0.0759	0.0659	0.0638	0.0605	0.0555	0.0546	0.0543	0.0533	0.0454
Rank	1	2	3	4	5	6	7	8	9	10	11
Area (Km^2)	55.69	54.78	183.25	141.93	15.53	88.18	18.73	41.42	74.54	83.83	71.09

SW Name	SW 16	SW 5	SW 17	SW 9	SW 22	SW 3	SW 20	SW 10	SW 6	SW 4	SW 21
FAHP Score	0.0437	0.0430	0.0324	0.0290	0.0287	0.0287	0.0269	0.0264	0.0211	0.0195	0.0125
Rank	12	13	14	15	16	17	18	19	20	21	22
Area (Km^2)	52.42	91.09	52.65	120.88	57.47	345.99	59.92	70.97	35.52	53.76	159.75

Table 6: Prioritized dryness-prone sub-watersheds based on Fuzzy-AHP score

SN.	Fuzzy-AHP Score	Priority Class	Total SWs	Sub Watersheds	Area (Sq. km.)	% Area
1	0.0681-0.0819	Very High	3	SW8, SW2, SW15	293.7187	15.22
2	0.0543-0.680	High	6	SW1, SW7, SW12, SW13, SW19, SW14	380.3315	19.71
3	0.0404-0.0542	Moderate	4	SW18, SW11, SW16, SW5	298.4241	15.47
4	0.0265-0.0403	Low	6	SW17, SW9, SW22, SW3, SW20, SW10	707.8735	36.69
5	≤ 0.0264	Very Low	3	SW6, SW4, SW21	249.0309	12.91
Total Area					1929.38	100.00

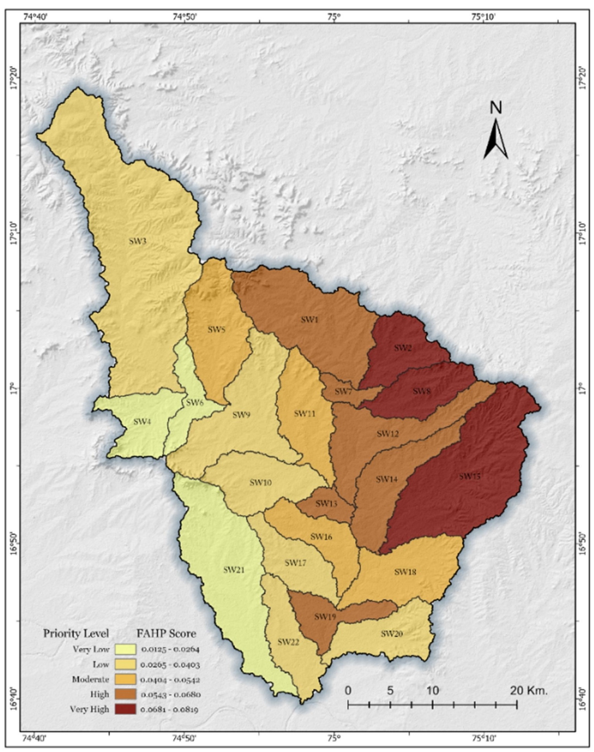

Figure 7: Prioritisation of the SWs for Climate Risk Mitigation based on Fuzzy-AHP

REFERENCES

[1] Abatzoglou JT, Dobrowski SZ, Parks SA, Hegewisch KC (2018) TerraClimate, a high-resolution global dataset of monthly climate and climatic water balance from 1958–2015. Sci Data 5:170191. https://doi.org/10.1038/sdata.2017.191

[2] Eichelberger S, McCaa J, … BN-NA, 2008 undefined Climate change effects on wind speed. 2162432711

[3] Flint LE, Flint AL (2012) Downscaling future climate scenarios to fine scales for hydrologic and ecological modeling and analysis. Ecol Process 1:2. https://doi.org/10.1186/2192-1709-1-2

[4] Jaiswal RK, Ghosh NC, Lohani AK, Thomas T (2015) Fuzzy AHP Based Multi Crteria Decision Support for Watershed Prioritization. Water Resour Manag 29:4205–4227. https://doi.org/10.1007/s11269-015-1054-3

[5] McVicar TR, Roderick ML, Donohue RJ, *et al* (2012) Global review and synthesis of trends in observed terrestrial near-surface wind speeds: Implications for evaporation. J. Hydrol. 416–417:182–205

[6] Prăvălie R, Sirodoev I, Patriche C, *et al* (2014) The analysis of the relationship between climatic water deficit and corn agricultural productivity in the Dobrogea plateau. Carpathian J earth Environ Sci 9:201–214

[7] Salmi T, Määttä A, Anttila P, *et al* (2002) Publications on air quality ATMOSPHERIC POLLUTANTS BY THE MANN-KENDALL. Finnish Meteorological Institute, Helsinki, Finland

[8] Sohoulande Djebou DC, Singh VP, Frauenfeld OW (2015) Vegetation response to precipitation across the aridity gradient of the southwestern United states. J Arid Environ 115:35–43. https://doi.org/10.1016/j.jaridenv.2015.01.005

[9] C.M. Thakar, S.S. Parkhe, A. Jain etal., 3d Printing: Basic principles and applications, Materials Today: Proceedings, https://doi.org/10.1016/j.matpr.2021.06.272

[10] Khan, R. M. I., Kumar, T., Supriyatno, T., &Nukapangu, V. (2021). The Phenomenon of Arabic-English Translation of Foreign

Language Classes During The Pandemic. IjazArabi Journal of Arabic Learning, 4(3). https://doi.org/10.18860/ijazarabi.v4i3.13597

[11] Sajja, G., Mustafa, M., Phasinam, K.,Kaliyaperumal, K., Ventayen, R., & Kassanuk, T. (2021). Towards Application of Machine Learning in Classification and Prediction of Heart Disease. 2021 Second International Conference On Electronics And Sustainable Communication Systems (ICESC).https://doi.org/10.1109/icesc51422.2021.9532940

[12] Veluri, R., Patra, I., Naved, M., Prasad, V.,Arcinas, M., Beram, S., & Raghuvanshi, A. (2021). Learning analytics using deep learning techniques for efficiently managing educational institutes. Materials Today:Proceedings. https://doi.org/10.1016/j.matpr.2021.11.416

[13] Yao J, Liu H, Huang J, *et al* (2020) Accelerated dryland expansion regulates future variability in dryland gross primary production. Nat Commun 11:1–10. https://doi.org/10.1038/s41467-020-15515-2.